ESKİŞEHİR TECHNICAL UNIVERSITY JOURNAL OF SCIENCE AND TECHNOLOGY
A- APPLIED SCIENCES AND ENGINEERING

Estuscience – Se, 2025, 26 (3) pp. 305 - 316, DOI: 10.18038/estubtda.1713749

RESEARCH ARTICLE

RUNWAY CONFIGURATION ANALYSIS BASED ON WIND DATA: A CASE STUDY OF WARSAW CHOPIN AIRPORT

Özlem ŞAHİN [1,*], Ali TATLI [2]

[1] Department of Air Traffic Control, Faculty of Aeronautics and Astronautics, Eskişehir Technical University, Eskişehir, Türkiye
ozlemsahin@eskisehir.edu.tr - 0000-0002-9632-5533

[2] Department of Aviation Electric and Electronics, Ali Cavit Çelebioğlu Civil Aviation School, Erzincan Binali Yıldırım University, Erzincan, Türkiye
ali.tatli@erzincan.edu.tr - 0000-0001-8925-8312

Abstract

Runway configuration at airports is determined based on the prevailing wind direction to ensure the safety of flight operations. In this process, wind direction, crosswind component, and wind coverage are of critical importance. In this study, Warsaw Chopin Airport, which has intersecting runways, is examined. Using 12 years of METAR data for the airport, wind speed, wind direction, and wind coverage were analyzed. Finally, monthly wind contour models were generated for the airport, and the relationship between wind and runway configuration was evaluated seasonally.

Based on the wind data from Warsaw Chopin Airport, it was found that the prevailing wind directions are west, northwest, and east-southeast; the average wind direction is 250°, while the maximum and minimum wind directions are 270° and 360°, respectively. Additionally, the wind coverage was calculated as 99.77% with the combined use of the existing intersecting runways, indicating that the current runway configurations are operationally highly sufficient.

Keywords

Aviation,
Airport,
Wind,
Runway Configuration,
Transportation

Time Scale of Article

Received : 04 June 2025
Accepted : 14 July 2025
Online date : 25 September 2025

1. INTRODUCTION

Wind direction and speed are critical factors in determining the optimal configuration of airport runways to ensure operational safety. Runways should be aligned to provide at least 95% usability without exceeding the permissible limits of the crosswind component. If a single runway configuration does not meet this criterion, alternative layouts—such as intersecting or crossing-extended runways—are considered. Crosswinds, particularly those blowing perpendicular (i.e., at 90°) to the runway, pose significant risks during takeoff and landing as they may cause aircraft to drift, skid, or lose control. When the crosswind component exceeds operational limits (typically between 10 and 20 knots), adjustments in runway configurations may become necessary. In airports with intersecting or crossing-extended runways, traffic can be directed to a more suitable runway. However, at airports with parallel runways, certain runways may need to be temporarily closed.

In addition to crosswinds, headwinds and tailwinds also significantly affect aircraft performance during takeoff and landing. Tailwinds—winds blowing in the same direction as the aircraft's flight path—increase required takeoff and landing distances, necessitating the use of longer runways and mandatory adjustments in performance data. Conversely, headwinds—winds blowing opposite to the direction of

*Corresponding Author: ozlemsahin@eskisehir.edu.tr

flight—enhance lift during takeoff, enabling aircraft to become airborne in shorter distances, and assist deceleration during landing by increasing drag [1,2].

When determining runway configurations, prevailing wind direction, crosswind limits, and wind coverage percentages must be considered together. Runways are typically oriented to maximize headwind components while minimizing the effects of crosswinds, thereby improving both the safety and efficiency of takeoff and landing operations. If crosswind limits are exceeded, runway changes are required at airports with multi-directional runways, whereas some runways may need to be deactivated at airports with parallel runway configurations. Aircraft may operate under tailwind conditions up to 5–10 knots; however, higher wind speeds necessitate runway changes [2].

Numerous studies have been conducted to forecast wind speed and direction. Various methods have been developed to predict local wind speed, often relying on stochastic models to accurately represent wind behavior [3-7]. Recent developments in the literature include the application of next-generation approaches—such as artificial intelligence, neural networks, and hybrid models—aimed at improving the accuracy and reliability of wind prediction [8-13]. Furthermore, studies focusing on runway orientation optimization have utilized various components such as crosswind effects, numerical analyses, machine learning techniques, and integrated airport operations [14-16]. For instance, Chang (2015) developed a model for optimizing multiple runway orientations based on crosswind data and validated its accuracy by comparing it with previous models [14]. Several studies have proposed optimization models to determine runway configurations under stochastic conditions [17-23]. Additionally, wind rose diagrams, which graphically illustrate how wind direction and speed are distributed over time at a given location, have become a widely used tool for summarizing large datasets and optimizing runway operations. Singh and Chopra (2012) developed a Java-based software on the NetBeans platform that enables the calculation of runway orientation and coverage ratios through wind rose analysis [24]. In another study conducted by Oktavia et al. (2023) at Minangkabau International Airport, ten years (2011–2020) of synoptic data obtained from a meteorological station were analyzed. The study identified the prevailing wind directions as southwest (203°–248°) with 41.97%, west (248°–293°) with 27.93%, and south (158°–203°) with 13.81%. The wind speeds were predominantly within the range of 4.08–7 knots (54.8%) [25]. The literature demonstrates substantial contributions to the field through studies on wind forecasting [3-9, 26-33], runway orientation optimization [14-23, 34-40] and wind rose applications [24,25].

In this study, Warsaw Chopin Airport, which features intersecting runways, has been selected as the case study. The objective is to examine the seasonal wind characteristics of the airport and evaluate their operational implications for runway usage. Meteorological data from the period 2010–2022 were analyzed using Python-based wind contour diagrams. The analysis assessed the seasonal frequency, adequacy, and efficiency of the existing runway configuration. This study comprehensively examines wind coverage based on possible runway configurations and seasonal wind contour diagrams.

2. METHODOLOGY

The International Civil Aviation Organization (ICAO) recommends that runway orientations be designed in accordance with prevailing wind directions to ensure the safe takeoff and landing of aircraft. Similarly, according to the standards of the Federal Aviation Administration (FAA), runway alignment should be planned to allow aircraft operations to be conducted without exceeding crosswind limits at least 95% of the time. ICAO and the European Union Aviation Safety Agency (EASA) define the Allowable Crosswind Component (ACC) based on the runway length required for takeoff. Accordingly, the crosswind limits are set at 10 knots (5.1 m/s) for runways shorter than 1200 meters, 13 knots (6.7 m/s) for runways shorter than 1500 meters, and 20 knots (10.3 m/s) for runways longer than 1500 meters. All these values are defined under dry runway surface conditions [41].

The FAA (2012) also specifies allowable crosswind components based on the Runway Design Code (RDC). The RDC consists of a letter and a Roman numeral. The letter represents the aircraft's approach speed (with "A" being the lowest and "E" the highest), while the Roman numeral indicates the aircraft's wingspan or tail height (with "I" denoting the smallest and "VI" the largest). Although visibility is also a factor considered in the RDC, it is not taken into account when determining the crosswind component. FAA standards [42] specify the allowable crosswind components corresponding to each RDC category.

The crosswind component limits are also supported by analyses derived from past accident data. For instance, van Es et al. (2001), based on statistical evaluations, concluded that a 15-knot crosswind threshold (including gusts) cannot be reduced without compromising safety. As such, many studies consider the 15-knot (7.7 m/s) value to represent the safe operational limit [1].

By decomposing the vector into its components, the influence of the wind can be examined by representing it in horizontal and vertical coordinates. To decompose wind vectors into directional components, a polar graph was utilized (Figure 1). Here, n represents the number of METAR reports, and V_1, V_2, ..., V_n denote the corresponding wind speeds. The horizontal and vertical vector components were calculated for all four trigonometric quadrants using trigonometric functions. These components were then summed along each axis to derive two resultant components, which together form the total wind vector.

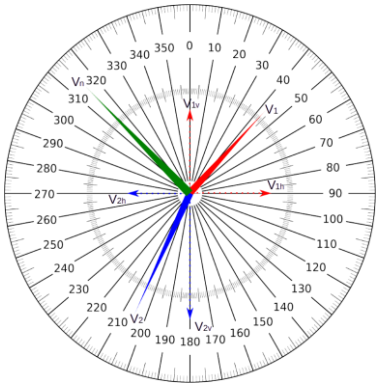

Figure 1. Coordinate system of wind vectors

The regions of the wind diagram's coordinate system are employed in the subsequent calculations, as expressed in Equations (1)–(4).

$$V_h = V \times sin\alpha \qquad V_v = V \times cos\alpha, \text{ if } 0°\leq\alpha\leq90° \quad (1)$$

$$V_h = V \times sin(180° - \alpha) \qquad V_v = -V \times cos(180° - \alpha), \text{ if } 90°\leq\alpha\leq180° \quad (2)$$

$$V_h = -V \times sin(\alpha - 180°) \qquad V_v = -V \times cos(\alpha - 180°), \text{ if } 180°\leq\alpha\leq270° \quad (3)$$

$$V_h = -V \times sin(360° - \alpha) \qquad V_v = V \times cos(360° - \alpha), \text{ if } 270°\leq\alpha\leq360° \quad (4)$$

$\boldsymbol{V_h}$; denotes the horizontal component of the wind speed vector (V), $\boldsymbol{V_v}$; denotes its vertical component, and α represents the angle of V amplitude wind.

2.1. The Calculation of Wind Coverage

According to the FAA (2012), runway configurations are required to ensure 95% annual wind coverage. Therefore, the crosswind component must remain within acceptable limits at least 95% of the time. If wind data analysis reveals that a single runway does not meet the 95% coverage criterion, the construction of a second runway in a different orientation (e.g., perpendicular) may be necessary to achieve the required total coverage. Similarly, EASA (2011) mandates that the runway number and

configuration must guarantee more than 95% usability for the aircraft in question. In this study, as in previous works [1], the allowable crosswind limit is assumed to be 15 knots.

Wind coverage refers to the period during which wind conditions fall within the defined crosswind and tailwind threshold values for a given runway. Excessive crosswinds may complicate aircraft maneuverability, while tailwinds can increase landing distances. Insufficient wind coverage can lead to flight cancellations and delays. To maximize wind coverage, airports optimize runway orientation or, if necessary, construct additional runways to improve coverage.

In tailwind and crosswind measurements, positive or negative values indicate wind direction. A positive tailwind value indicates wind pushing the aircraft from behind, while a negative tailwind (i.e., headwind) indicates wind coming from the front. A positive crosswind value means the wind is blowing from the right to the left, whereas a negative value indicates wind from the left to the right [43,44]. Tailwind (or headwind) and crosswind components can be calculated using Equations (5) and (6), respectively.

$$W_{T/H} = V \times cos(\theta) \quad (5)$$

$$W_C = V \times sin(\theta) \quad (6)$$

where $\boldsymbol{W_{T/H}}$ is the tail/head winds and $\boldsymbol{W_C}$ is the crosswind components, V is the speed of wind and θ represents the angular disparity between the runway orientation and the wind direction. Wind coverage calculation is given (7).

$$\boldsymbol{WC = \left(1 - \frac{T_U}{T_{TOTAL}}\right) \times 100} \quad (7)$$

where $\boldsymbol{WC}$ signifies the wind coverage in percent, $\boldsymbol{T_U}$ is the runway unavailability time, and the $\boldsymbol{T_{TOTAL}}$ is the total time [45].

3. RESULTS

Warsaw Chopin Airport, which has two intersecting runways—Runway 11/29 (2800 meters) and Runway 15/33 (3690 meters) (Figure 2)—is a major airport that experienced a significant increase in traffic in 2023. According to statistics from May 2025, the airport handles approximately 600 aircraft movements per day. This airport was selected for analysis due to its unique feature of having only two intersecting runways with a 40-degree difference in orientation.

The configuration of intersecting runways at airports is typically determined based on crosswind components, and it is generally observed that these configurations are arranged with an angular difference of 60° or more. For instance, Amsterdam Schiphol Airport has intersecting runways 36/18 and 09/27; Brussels Airport has 07/25 and 01/19; and Zurich Airport features 10/28 and 16/34. Although there is no strict rule regarding the angle between runways, a 60° difference is commonly seen. However, in cases of high crosswind intensity, alternative configurations with different intersecting angles are certainly possible.

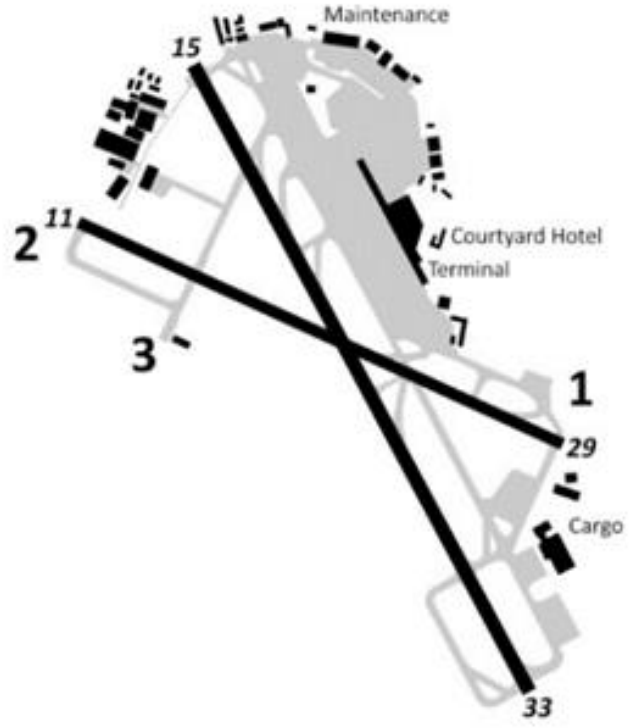

Figure 2. Runway configuration diagram for Warsaw Chopin Airport [46]

For this airport, a total of 241,284 METAR-coded wind data records from the years 2010 to 2022 were processed. Among these, 2,410 entries were identified as missing data, representing approximately 1% of the entire dataset. Additionally, 18,023 records reported wind speeds below 1 knot and were excluded from the analysis, as such cases were considered calm wind conditions. In total, 238,874 data entries were analyzed.

Based on the cumulative frequency distribution over the 12-year period, it was observed that the wind predominantly blew from directions between 260°–310° and 100°–140° (Figure 3). The average wind direction was found to be 250°, with the most frequently occurring wind direction (mode) being 270°, and the minimum observed direction being 360° (Figure 4).

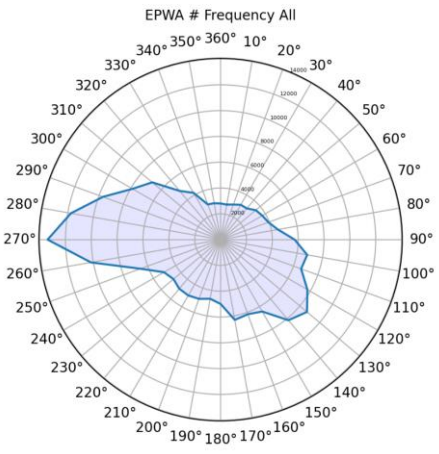

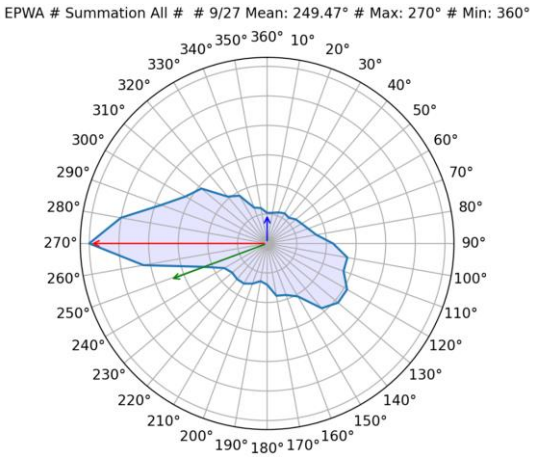

Figure 3. Total wind frequency in directions **Figure 4.** Average, minimum and maximum wind direction in total

In this study, to evaluate the usability of the existing runways, wind coverage was first analyzed—i.e., whether the current runway configuration allows for more than 95% operational usability under the defined crosswind and tailwind threshold conditions. When runway 15/33 was evaluated individually, the wind coverage was calculated as 97.92%. For runway 11/29, the wind coverage was found to be 99.26%. When both runways were considered for joint use, wind coverage increased to 99.77%.

These results indicate that the combined use of both runways significantly enhances wind coverage. The current runway configuration is highly sufficient, allowing for safe flight operations in 99.77% of wind conditions, thereby meeting both FAA and EASA requirements. Therefore, it can be concluded that the existing runway system at this airport is adequate and there is no need for the construction of an additional runway (Table 1). Table 1 discusses wind coverage based on possible cross-runway configurations of row and column intersections.

Table 1. The wind coverage for all runway configurations

		Runway Configuration																
		36/18	**01/19**	**02/20**	**03/21**	**04/22**	**05/23**	**06/24**	**07/25**	**08/26**	**09/27**	**10/28**	**11/29**	**12/30**	**13/31**	**14/32**	**15/33**	**16/34**	**17/35**
Runway Configuration	**36/18**	%95.82																	
	01/19	%96.31	%95.44																
	02/20	%96.68	%96.14	%95.48															
	03/21	%97.28	%96.74	%96.32	%95.77														
	04/22	%98.02	%97.48	%97.06	%96.77	%96.36													
	05/23	%98.77	%98.23	%97.81	%97.51	%97.31	%97.02												
	06/24	%99.17	%98.95	%98.53	%98.23	%98.03	%97.89	%97.65											
	07/25	%99.50	%99.28	%99.14	%98.85	%98.64	%98.50	%98.39	%98.20										
	08/26	%99.72	%99.58	%99.45	%99.35	%99.15	%99.01	%98.90	%98.81	%98.67									
	09/27	%99.92	%99.78	%99.71	%99.61	%99.55	%99.41	%99.30	%99.21	%99.13	%98.98								
	10/28	%99.95	%99.94	%99.87	%99.83	%99.77	%99.73	%99.62	%99.53	%99.45	%99.35	%99.20							
	11/29	%99.92	%99.92	%99.94	%99.90	%99.88	%99.84	%99.81	%99.73	%99.65	%99.54	%99.44	**%99.26**						
	12/30	%99.78	%99.81	%99.84	%99.90	%99.87	%99.91	%99.88	%99.86	%99.78	%99.68	%99.58	%99.44	%99.16					
	13/31	%99.51	%99.55	%99.61	%99.67	%99.83	%99.87	%99.94	%99.92	%99.90	%99.79	%99.69	%99.56	%99.35	%98.94				
	14/32	%99.00	%99.16	%99.23	%99.37	%99.53	%99.83	%99.90	%99.96	%99.93	%99.90	%99.80	%99.67	%99.45	%99.11	%98.53			
	15/33	%98.29	%98.45	%98.82	%98.96	%99.28	%99.59	%99.88	%99.94	%99.96	%99.93	%99.90	**%99.77**	%99.55	%99.21	%98.69	**%97.92**		
	16/34	%97.51	%97.67	%98.04	%98.64	%98.97	%99.39	%99.68	%99.91	%99.93	%99.96	%99.93	%99.87	%99.66	%99.31	%98.80	%98.08	%97.19	
	17/35	%96.76	%96.92	%97.29	%97.89	%98.63	%99.05	%99.45	%99.68	%99.91	%99.93	%99.96	%99.89	%99.75	%99.40	%98.89	%98.18	%97.40	%96.41

3.1. Winter Season

During the winter season, prevailing wind directions for December, January, and February were observed to be around 270° (Figure 5). It can be stated that wind speeds increased in January and February, reaching up to 25 knots. In December, the dominant wind direction remained at 270°, with additional wind activity from 90° to 140° reaching a maximum of 18 knots. However, in January and

February, in addition to the dominant westerly winds, stronger easterly and southeasterly winds were also recorded, with speeds reaching approximately 20–25 knots. Given the runway configuration of 11/29 and 15/33, it is clearly observed that runway 11/29 is the most frequently used configuration during the winter season.

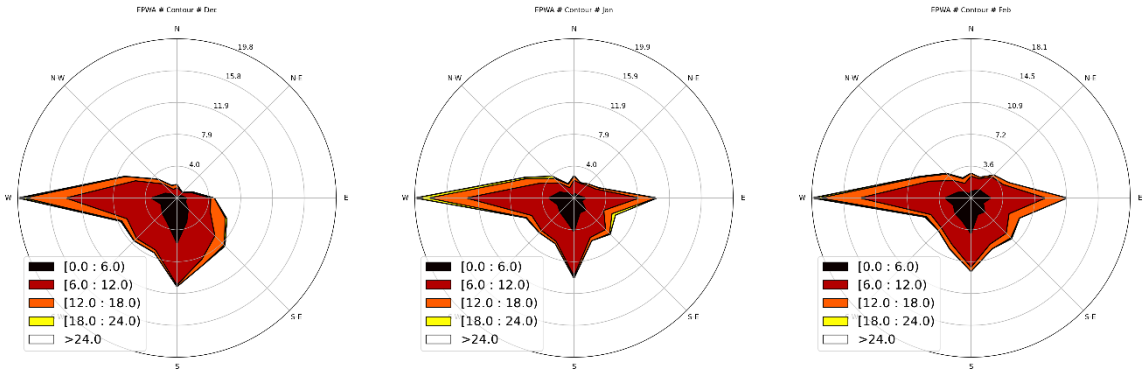

Figure 5. Wind contour diagrams for December, January, February

3.2. Spring Season

In the spring season, it was observed that the wind continued to blow predominantly from the prevailing direction; however, in April and May, it intensified and shifted towards the north (Figure 6). In March, wind speeds reached up to 25 knots between 270° and 310°, and similar wind speeds were recorded between 270° and 360° in April. Under these conditions, the most frequently used runway headings are expected to be 29 and 31. Additionally, winds reaching up to 25 knots were also observed between 90° and 125°. Consequently, runway headings 11 and 15 would also be actively utilized due to experiencing approximately 20–25 knots of headwind. In May, winds of 25 knots were again recorded from 270°–310°, and the easterly winds observed in April continued to exert their influence. Overall, strong northwesterly and southeasterly winds were dominant during the spring season.

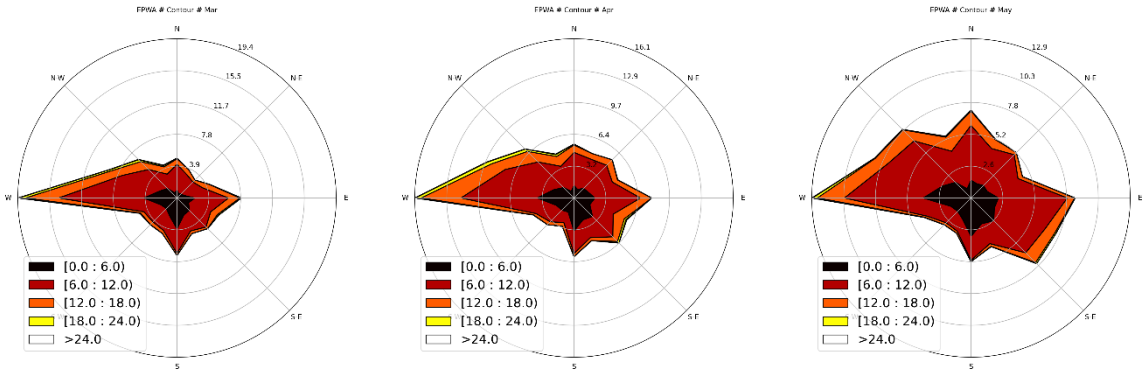

Figure 6. Wind contour diagrams for March, April, May

3.3. Summer Season

In June and July, winds blowing from 270°–360° exhibited a reduced intensity compared to spring and winter seasons, with speeds ranging between 18–20 knots (Figure 7). Although southeast winds of approximately 20 knots were observed in June, the influence of winds from this direction was not

significant in July and August. In the case of 20-knot winds from 100°–120° in June, runway 11 would be the preferred runway heading. Runway 15, however, would not be preferred due to exposure to approximately 16 knots of crosswind. For winds blowing from 270°–310° at 20 knots, runways 33 and 29 are expected to be utilized, as they provide approximately 20 knots of headwind. In the case of 20-knot winds from 320°–360°, runway 33 would be actively used. Winds from this direction would result in crosswinds of approximately 18 knots on runways 11 and 29, exceeding the operational limit, rendering these runways unusable.

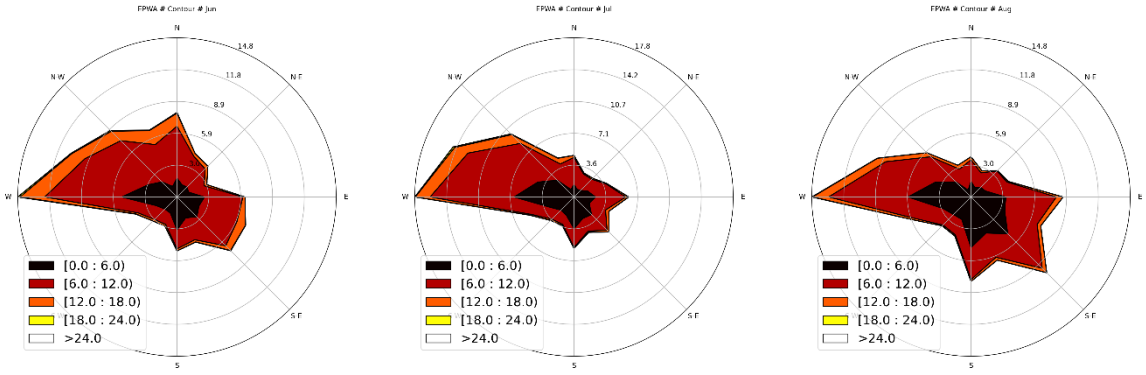

Figure 7. Wind contour diagrams for June, July, August

3.4. Autumn Season

In autumn, the prevailing wind directions, namely west, northwest (270°–360°), and east-southeast (90°–120°), were observed to maintain an intensity of approximately 20 knots (Figure 8). During this season, all available runways at the airport were actively utilized based on wind direction and speed. For northwest winds, runway headings 29 and 33 were actively employed. Notably, in November, winds from 90°–120° were observed to be more dominant. In the case of 20-knot winds from 90°–120°, runway 11 was actively used. For easterly winds, the runway 15/33 configuration was exposed to full crosswinds (17 knots) and tailwinds (10 knots), rendering it unusable.

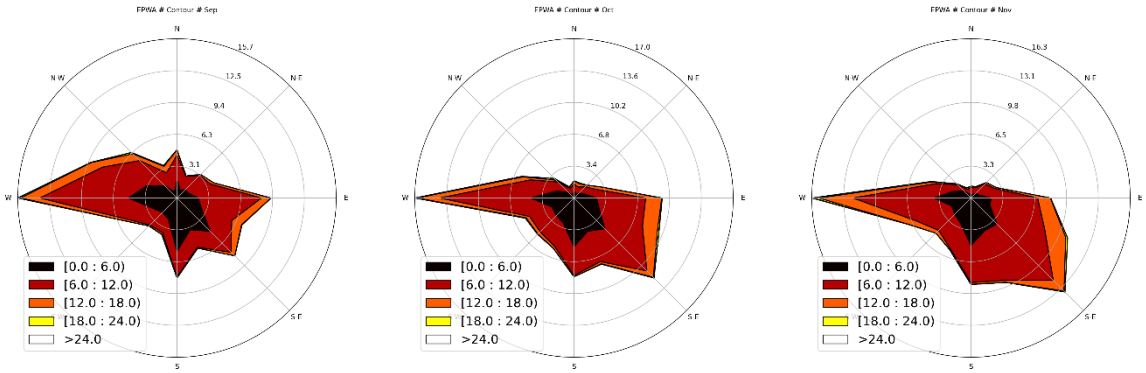

Figure 8. Wind contour diagrams for September, October, November

4. CONCLUSION

This study aims to analyze the relationship between runway configuration and seasonal wind characteristics at Warsaw Chopin Airport using 12 years of METAR data (2010–2022). The results indicate that the combined use of the existing 11/29 and 15/33 runway configurations achieves a wind coverage rate of 99.77%, significantly exceeding the minimum 95% coverage requirement set by ICAO and FAA. This demonstrates that the airport's current runway infrastructure is operationally sufficient across all seasons.

Analyses reveal distinct variations in wind direction and intensity across different seasons. In winter, westerly winds around 270° intensify, reaching up to 25 knots, particularly in January and February. Under these conditions, the 11/29 runway is predominantly utilized. In spring and autumn, wind directions fluctuate between northwest and southeast, while in summer, wind intensity decreases and exhibits a more variable directional distribution. This variability allows flexibility in runway selection; however, during periods of intensified easterly winds, the 15/33 runway approaches or exceeds operational limits.

The data also indicate no significant wind impact from northeast or southwest directions, suggesting no need for runway configurations aligned with these directions. This finding confirms that the current runway configurations are optimized for prevailing wind directions, ensuring operational efficiency.

The study's findings highlight the high adaptability of intersecting runway configurations to seasonal wind variability. Similar studies in the literature also note that multiple runway configurations effectively enhance wind coverage [14,24]. At Warsaw Chopin Airport, intersecting runway configurations increase operational flexibility and support the sustainability of safe flight operations.

In conclusion, the intersecting runway structure at Warsaw Chopin Airport demonstrates high adaptability to seasonal wind variability, enhancing operational flexibility and supporting flight safety and efficiency. Future studies incorporating additional environmental variables affecting runway usability (e.g., fog, precipitation, runway surface conditions) could provide a more comprehensive evaluation. Such studies can also contribute significantly to sustainable airport operations and infrastructure planning tailored to meteorological conditions.

CONFLICT OF INTEREST

The authors stated that there are no conflicts of interest regarding the publication of this article.

CRediT AUTHOR STATEMENT

Özlem Şahin: Conceptualization, Investigation, Writing - Original Draft, Visualization, Supervision, Validation, Writing - Review & Editing. **Ali Tatlı:** Conceptualization, Methodology, Software, Formal analysis, Data Curation, Investigation, Writing - Review & Editing.

REFERENCES

[1] Bellasio R. Analysis of wind data for airport runway design. J. Airl. Airport Manag. 2014; 4(2): 1–15.

[2] Maslovara A, Mirkovic B. Impact of tailwind on airport capacity and delay at Zurich Airport. Transp. Res. Procedia 2021; 59: 117–126.

[3] Hernández-Romero E, Valenzuela A, Rivas D. Probabilistic multi-aircraft conflict detection and resolution considering wind forecast uncertainty. Aerosp. Sci. Technol. 2020; 105: 105973.

[4] Dönmez K, Cetek C, Kaya O. Air traffic management in parallel-point merge systems under wind uncertainties. J. Air Transp. Manag. 2022; 104: 102268.

[5] Gu Y, Rhudy MB. Stochastic wind modeling and estimation for unmanned aircraft systems. In: AIAA Aviation Forum; 2019.

[6] Rodionova O, Sridhar B, Ng HK. Conflict resolution for wind-optimal aircraft trajectories in North Atlantic Oceanic Airspace with wind uncertainties. In: IEEE/AIAA Digital Avionics Systems Conference; 2016. pp. 1–10.

[7] Vela AE, Salaun E, Solak S, Feron E. A two-stage stochastic optimization model for air traffic conflict resolution under wind uncertainty. In: IEEE/AIAA Digital Avionics Systems Conference; 2009. pp. 1–10.

[8] Saeed A, Li C, Gan Z, Xie Y, Liu F. A simple approach for short-term wind speed interval prediction based on independently recurrent neural networks and error probability distribution. Energy 2022; 238: 122012.

[9] Chen G, Tang B, Zeng X, Zhou P, Kang P, Long H. et al. Short-term wind speed forecasting based on long short-term memory and improved BP neural network. Int. J. Electr. Power Energy Syst. 2022; 134: 107365.

[10] Wang Y, Zhang N, Wu L, Wang Y. Wind speed forecasting based on the hybrid ensemble empirical mode decomposition and GA-BP neural network method. Renew. Energy 2016; 94: 629–636.

[11] Zhang Y, Chen B, Pan G, Zhao Y. A novel hybrid model based on VMD-WT and PCA-BP-RBF neural network for short-term wind speed forecasting. Energy Convers. Manag. 2019; 195: 180–197.

[12] Valdivia-Bautista SM, Domínguez-Navarro J. A, Pérez-Cisneros M, Vega-Gómez CJ, Castillo-Téllez B. Artificial intelligence in wind speed forecasting: A review. Energies 2023; 16(5): 2457.

[13] Dong X, Li C, Shi H, Zhou P. Short-term probabilistic wind speed predictions integrating multivariate linear regression and generative adversarial network methods. Atmosphere 2024; 15(3): 294.

[14] Chang SW. Crosswind-based optimization of multiple runway orientations. J. Adv. Transp. 2015; 49(1): 1–9.

[15] Barea A, Celis R, Cadarso L. An integrated model for airport runway assignment and aircraft trajectory optimisation. Transp. Res. C Emerg. Technol. 2024; 160: 104498.

[16] Kalyanam KM, Memarzadeh M, Crissman J, Yang, R, Tejasen KT Applying machine learning tools for runway configuration decision support. In: International Conference on Research in Air Transportation; 2024.

[17] Herrema F, Curran R, Hartjes S, Ellejmi M, Bancroft S, Schultz M. A machine learning model to predict runway exit at Vienna airport. Transp. Res. E Logist. Transp. Rev. 2019; 131: 329–342.

[18] Oktal H, Yildirim N. New model for the optimization of runway orientation. J. Transp. Eng. 2014; 140(3): 04013020.

[19] Oktal H, Yıldırım N. Optimisation of runway orientations for three-runway configurations. Aeronaut. J. 2016; 120(1233): 1693–1709.

[20] Mousa RM, Mumayiz SA. Optimization of runway orientation. J. Transp. Eng. 2000; 126(3): 228–236.

[21] Ahmed MS, Alam S, Barlow M. A cooperative co-evolutionary optimisation model for best-fit aircraft sequence and feasible runway configuration in a multi-runway airport. Aerospace 2018; 5(3): 85.

[22] Provan CA, Atkins SC. Optimization models for strategic runway configuration management under weather uncertainty. In: AIAA Aviation Technology, Integration and Operations Conference; 2010.

[23] Li L, Clarke JP, Chien HHC, Melconian T. A probabilistic decision-making model for runway configuration planning under stochastic wind conditions. In: IEEE/AIAA Digital Avionics Systems Conference; 2009. pp. 3–A.

[24] Singh M, Chopra T. Use of computer applications for determining the best possible runway orientation using wind rose diagrams. In: International Conference on Recent Trends in Transportation, Environmental and Civil Engineering; 2012. pp. 1–6.

[25] Oktavia S, Syafriani D, Dwiridal L, Sudiar NY. Analysis of surface wind speed at Minangkabau International Airport for the period 2011–2020 using the windrose method. J. Phys. Conf. Ser. 2023; 2582(1): 012006.

[26] Han S, Park B, Lee H. Analysis of the impacts of wind on final approach overshoot using historical flight and weather data. In: AIAA SciTech Forum; 2024. pp. 1–10.

[27] Tatli A, Suzer AE, Filik T, Karakoc TH. A case study on investigating probabilistic characteristics of wind speed data for green airport. In: Solutions for Maintenance Repair and Overhaul, ISATECH 2021; Springer, Cham; 2024. pp. 1–15.

[28] Sardjono W, Kusnoputranto H, Soesilo TEB, Utama DN, Sudirwan J. Study of runway crosswind and tailwind potential for airport sustainability: A study of Soekarno Hatta airport, Cengkareng, Indonesia. In: IOP Conf. Ser. Earth Environ. Sci. 2021; 729(1): 012012.

[29] Maslovara A, Mirković B. Impact of tailwind on airport capacity and delay at Zurich Airport. Transp. Res. Procedia 2021; 59: 117–126.

[30] O'Connor A, Kearney D. Evaluating the effect of turbulence on aircraft during landing and take-off phases. Int. J. Aviat. Aeronaut. Aerosp. 2018; 5(4): 10.

[31] Le Y, Li Y, Zhang Y. Impact of runway surface wind on afternoon and night flight operation at Linzhi Airport. Ind. Eng. Innov. Manag. 2022; 56: 48–58.

[32] Prema V, Rao KU. Time series decomposition model for accurate wind speed forecast. Renew Wind Water Sol 2015; 2: 18.

[33] Schlink U, Tetzlaff G. Wind speed forecasting from 1 to 30 minutes. Theor Appl Climatol 1998; 60: 191–198.

[34] Dhal R, Roy S, Tien SL, Taylor C, Wanke C. Operationally structured model for strategic runway configuration predictions. J Air Transp 2019; 27(2): 96–108.

[35] Wang Y, Zhang Y. Prediction of runway configurations and airport acceptance rates for multi-airport system using gridded weather forecast. Transp Res C Emerg Technol 2021; 125: 103049.

[36] Lau MEC, Lam AJG, Alam S. Predicting runway configuration transition timings using machine learning methods. In: 2021 Winter Simulation Conference (WSC); 13–15 Dec 2021; Phoenix, AZ, USA. New York, NY, USA: IEEE. pp. 1–12.

[37] Alves D, Mendonça F, Mostafa SS, Morgado-Dias F. Deep learning enhanced wind speed and direction forecasting for airport regions. Weather Forecast 2025; 40(1): 207–221.

[38] Taufiq LC, Putri A, Apriandy F. Simplified spatial wind vector interpolation method for airport runway orientation analysis. E3S Web Conf 2024; 476: 01057.

[39] Shankar A, Sahana BC. Efficient prediction of runway visual range by using a hybrid CNN-LSTM network architecture. Theor Appl Climatol 2024; 155(3): 2215–2232.

[40] Andy LJG, Alam S, Lilith N, Piplani R. A deep reinforcement learning approach for runway configuration management. J Air Transp Manag 2024; 120: 102672.

[41] International Civil Aviation Organization. Aerodromes—Annex 14 to the Convention on International Civil Aviation: Aerodrome Design and Operations, 3rd ed., vol. 1, 1999.

[42] Ashford N, Wright PH. Airport Engineering, 3rd ed. Hoboken, NJ, USA: Wiley; 1992.

[43] International Civil Aviation Organization. Annex 14 to the Convention on International Civil Aviation: Aerodrome Design and Operations, 7th ed., 2018.

[44] Baimukhametov G, White G. Review and improvement of runway friction and aircraft skid resistance regulation. Appl Sci 2025; 15(2): 548.

[45] Federal Aviation Administration. Advisory Circular 150/5300-13A: Airport Design. Washington, DC, USA: U.S. Department of Transportation; 2022.

[46] https://acukwik.com/Airport-Info/icao/epwa last accessed 2025/06/02